# Divertor Detachment with Multi-Species Impurity Seeding in LHD*)

Kiyofumi MUKAI[1,2), Suguru MASUZAKI[1)], Yuki HAYASHI[1)], Tetsutaro OISHI[1,2)], Chihiro SUZUKI[1)], Masahiro KOBAYASHI[1,2)], Hirohiko TANAKA[3)], Byron J. PETERSON[1,2)] and the LHD Experiment Group[1)]

[1)]*National Institute for Fusion Science, National Institutes of Natural Sciences, Toki 509-5292, Japan*
[2)]*The Graduate University for Advanced Studies, SOKENDAI, Toki 509-5292, Japan*
[3)]*Graduate School of Engineering, Nagoya University, Nagoya 464-8603, Japan*

(Received 20 April 2020 / Accepted 2 June 2020)

Divertor detachment using higher-Z (Kr) and/or lower-Z (Ne) is investigated. Using Kr+Ne superimposed seeding, plasma radiation could be enhanced at the upstream region in the edge plasma with suppression of impurity accumulation toward the core plasma. Here, the pre-seeded Kr emission was drastically enhanced after the subsequent Ne seeding. Moreover, the detachment using Kr+Ne seeding could be stably sustained while the detachment using single species seeding is short-lived. Reduction of edge electron temperature due to Ne seeding can promote the Kr emission at the upstream region. It indicates the availability of multi-species impurity seeding with different cooling rate.



Keywords: divertor detachment, impurity seeding, stable sustainment, superimposed seeding, radiation profile

DOI: 10.1585/pfr.15.1402051

## 1. Introduction

Divertor detachment using impurity seeding is one of the effective operation scenarios to reduce divertor heat loads to lower than 10 MW/m$^2$ in ITER and fusion reactors. To manage the huge power exhaust, radiation enhancement is required not only in the divertor region but also in the upstream region along with suppression of core plasma dilution. Using impurity seeding with a single species, it is difficult to realize such radiation enhancement in a wide region. Therefore, multi species impurity seeding is proposed in JT-60SA [1]. Moreover, it is predicted by the COREDIV code that additional Kr seeding is effective for divertor detachment [2]. In the Large Helical Device (LHD), we have investigated detachment using Ne or Kr seeding individually [3–6] and using resonant magnetic perturbation (RMP) [7]. In the Ne seeded plasmas, both radiation enhancement in the ergodic region and divertor heat load reduction were observed. It is reproduced well by the three-dimensional transport code EMC3-EIRENE [8]. On the other hand, in the Kr seeded plasmas, plasma radiation moved from the edge to the core region gradually. Moreover, reduction of the divertor heat load was not significant. However, the radial profile of the plasma radiation was not discussed and superimposed seeding of impurities have not been investigated. Therefore, in this study, we tried superimposed seeding using Kr and Ne as a comparison with puff amount scan with only Ne seeding. To enhance plasma radiation not only in the divertor region but also in the upstream region, seeded impurities should radiate in wide electron temperature, $T_e$, region. Impurity seeding using higher-Z and lower-Z is effective for the radiation in the wide $T_e$ region. Since the cooling rate of Ne reaches a maximum at $T_e \sim 30$ eV while the rate of Kr has a local minimum at $T_e \sim 30$ eV, it is expected that these impurities could enhance plasma radiation complementarity. In this paper, characteristics of the divertor detachment using only Ne seeding are described in Sec. 2. Plasma behavior in only Kr seeded plasmas is shown in Sec. 3. Characteristics of the divertor detachment using superimposed seeding of Kr and Ne are described in Sec. 4. The paper is summarized in Sec. 5.

## 2. Divertor Detachment Using Ne Seeding

Figure 1 shows the waveform in divertor detachment using Ne seeding. In this study, the standard magnetic configuration with cancellation of the error field was used, which position of magnetic axis, $R_{ax}$, is 3.60 m, and toroidal magnetic field is 2.75 T. The direction of the magnetic field was counterclockwise. Plasma was generated by electron cyclotron heating and was sustained by three neutral beam injections (NBIs) of tangential injection. Ne was seeded from 4.1 s for 50 ms. The seeded Ne amount was estimated to be 0.09 Pa·m$^3$. Total plasma radiation, $P_{rad}$, started to increase after Ne injection, then after $\sim 0.2$ s $P_{rad}$

*author's e-mail: mukai.kiyofumi@nifs.ac.jp*
*) This article is based on the invited talk at the 36th JSPF Annual Meeting (2019, Kasugai).

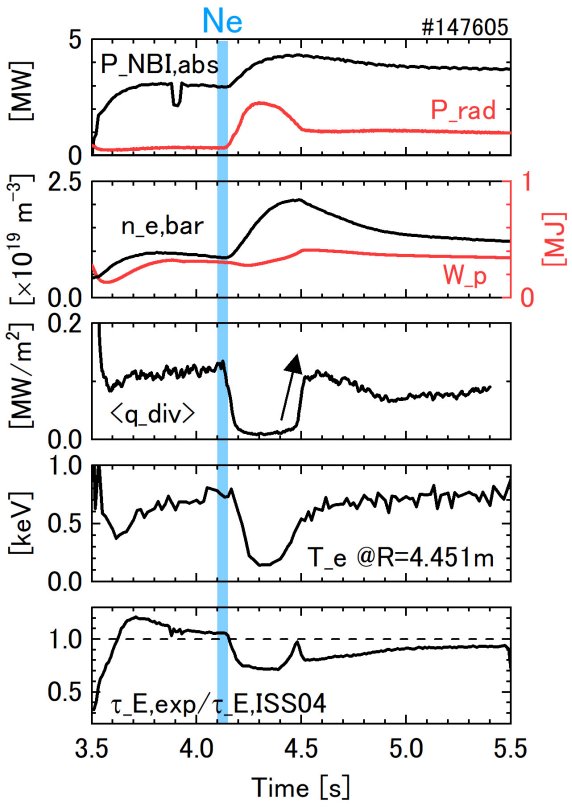


Fig. 1 Divertor detachment using Ne seeding. $f_{\rm rad} = P_{\rm rad}/P_{\rm NBI}$ reached 56% transiently. $\langle q_{\rm div}\rangle$ gradually decreased by $\sim$ 90%. $\tau_{\rm E,exp}/\tau_{\rm E,ISS04}$ is > 0.7. 0.4 s after the Ne seeding, the plasma was reattached with increase of edge $T_{\rm e}$ and reduction of $P_{\rm rad}$.

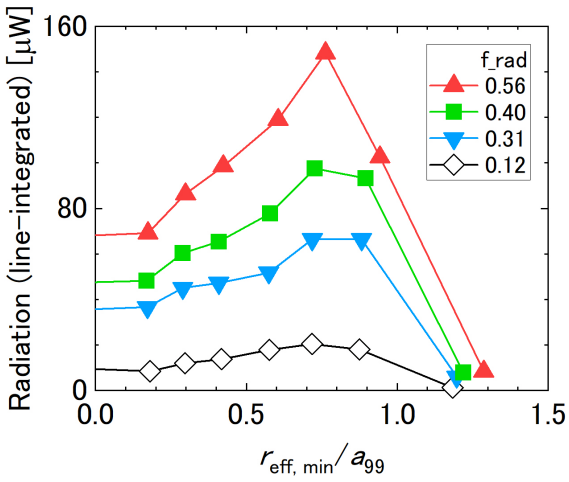


Fig. 2 $f_{\rm rad}$ dependence of radiation profile. Radiation was enhanced at upstream region ($r_{\rm eff,min}/a_{99} \sim 0.8$) with increase of $f_{\rm rad}$.

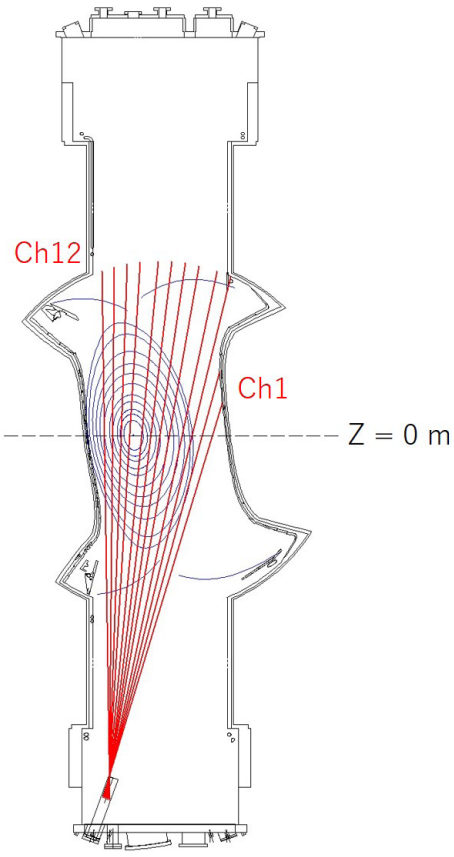


Fig. 3 Sightlines of resistive bolometer arrays.

reached the maximum. Here, line-averaged electron density, $n_{\rm e,bar}$, increased due to the Ne ionization and change of wall recycling. Although NBI port-through power is constant, NBI absorption power ($P_{\rm NBI,abs}$) increased with increasing $n_{\rm e,bar}$ due to the increase in heating efficiency. Divertor heat flux is measured with Langmuir probe arrays located in 7 of 10 toroidal sections. Toroidally averaged heat flux, $\langle q_{\rm div}\rangle$, decreased by $\sim$ 90% with the $P_{\rm rad}$ enhancement. During the detachment, $\tau_{\rm E,exp}/\tau_{\rm E,ISS04}$ is > 0.7. Here, $\tau_{\rm E,exp}$ and $\tau_{\rm E,ISS04}$ are energy confinement time evaluated by the experiment and ISS04 scaling, respectively [9]. Figure 2 shows the maximum radiation fraction ($f_{\rm rad} = P_{\rm rad}/P_{\rm NBI,abs}$) dependence of the radiation profile. The radiation profile was measured by resistive bolometer arrays with sightlines shown in Fig. 3. Here, $r_{\rm eff,min}$ is the minimum of effective minor radius on each sightline. $a_{99}$ is the averaged minor radius in which 99% of the electron stored energy is confined. $f_{\rm rad} \sim 12\%$ corresponds to a background discharge without Ne seeding. The $f_{\rm rad}$ increased with the increase of the puff amount. When $f_{\rm rad}$ was 31% and 40%, the plasma radiation from the edge plasma ($0.7 < |r_{\rm eff,min}/a_{99}| < 0.9$) increased. Furthermore, when $f_{\rm rad}$ was 56%, the radiation profile enhanced at the upstream of the edge plasma ($0.7 < |r_{\rm eff,min}/a_{99}| < 0.8$). However, the detachment disappeared 0.4 s after the Ne seeding. Figure 4 shows the time evolution of the NeVIII emission radial profile measured by EUV spectroscopy [10]. NeVIII or lower charge states can be considered as the dominant radiator since $T_{\rm e}$ at $0.8 < |r/r_{\rm LCFS}| < 1.0$ where plasma radiation mainly occurred is lower than the NeIX ionization energy of 1195.3 eV. The seeded Ne pen-

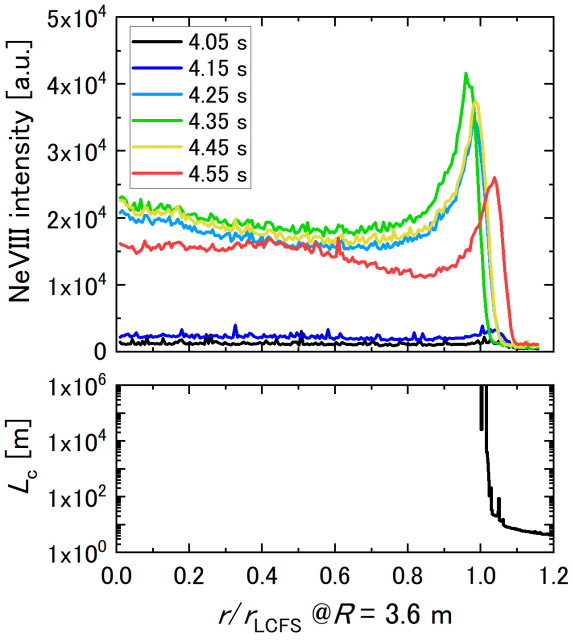


Fig. 4 Time evolution of NeVIII emission radial profile and radial profile of connection length. The seeded Ne penetrated the LCFS and then moved outward.

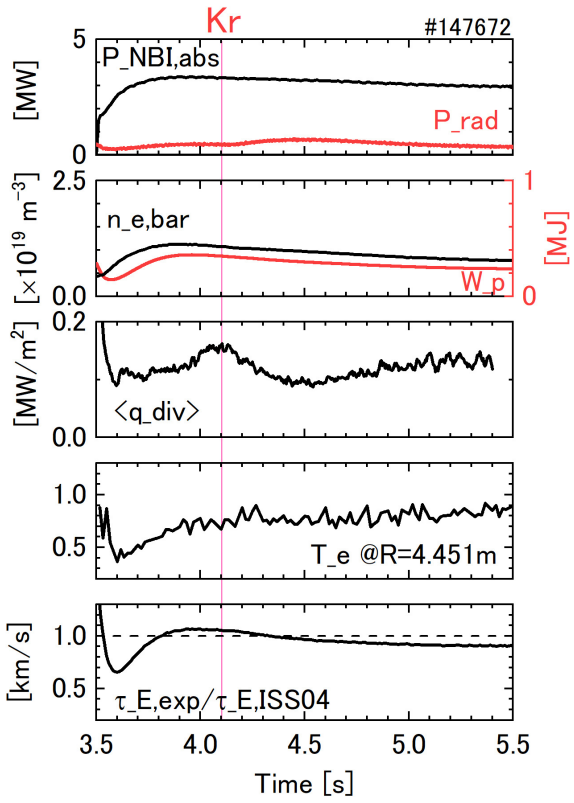


Fig. 5 Divertor detachment using Kr seeding. Plasma response was much slower than the case of only Ne seeding. The maximum $f_{rad}$ ~ 21% was observed at 4.5 s. Here, $\langle q_{div} \rangle$ gradually decreased by ~ 43% but reduction of edge Te was not observed. $\tau_{E,exp}/\tau_{E,ISS04}$ is > 0.9.

etrated into the last closed flux surface (LCFS) where the connection length, $L_c$, clearly increased as shown in Fig. 4. The Ne reached the innermost position at 4.35 s, then, the Ne moved outward. Since the emission intensity is a line-integrated value measured by EUV spectroscopy, the intensity from the core region shown in Fig. 4 should be strongly affected by edge emission. The outward shift of NeVIII emission region occurred by the increase of edge $T_e$ due to the improvement of the NBI heating efficiency as shown in Fig. 1. The shift leads the reduction of radiative cooling and the reattachment finally. In order to sustain the detachment, multi-pulse seeding is a candidate, but it is not easy since the reattached plasma shown in Fig. 1 is different from the plasma before the Ne seeding. Density control using further pumping might be helpful. Multi pulses using moderate Ne seeding could sustain the detachment with $f_{rad}$ ~ 30% [3].

## 3. Plasma Behavior in Kr Seeded Plasmas

Figure 5 shows the waveform in Kr seeded plasma. Kr was seeded from 4.1 s for 8 ms. The seeded Kr amount was estimated to be 0.02 Pa·m$^3$. The plasma response was much slower than the case of only Ne seeding. $P_{rad}$ slightly increased after Kr injection and reached a maximum at 4.5 s. Here, $f_{rad}$ was ~ 21%. $\langle q_{div} \rangle$ gradually decreased by ~ 43%. $\tau_{E,exp}/\tau_{E,ISS04}$ is > 0.9. Kr seeding with an increased amount induced radiative collapse. Seeding with higher-Z seems to be effective for enhancing the radiation toward the upstream region. However, higher-Z impurities have lower first ionization energy. The first ionization energies of Ne and Kr was 21.6 eV and 14.0 eV, respectively. Thus, higher-Z impurities are ionized in the more downstream region in the ergodic layer where the friction force is dominant.

## 4. Divertor Detachment Using Kr+Ne Superimposed Seeding

Kr and Ne superimposed seeding could overcome the limitation of the higher-Z seeding. Figure 6 shows the waveform in Kr and Ne superimposed seeded plasma. Kr was seeded at 4.1 s for 5 ms and Ne was seeded 0.4 s after the Kr seeding since the response of Kr is slower than Ne. The seeded amounts of Kr and Ne were 0.02 Pa·m$^3$ and 0.05 Pa·m$^3$, respectively. After Ne seeding, the plasma was detached and it was sustained for ~ 1 s. Further extension of the sustainment can be achievable if there is no limitation on the NBI pulse length since the plasma was ended by the termination of NBI heating. $f_{rad}$ was ~ 40% which is 10% higher than the previous sustainement using multi-pulse Ne seeding [3]. $\langle q_{div} \rangle$ decreased by ~ 90% compared with the $\langle q_{div} \rangle$ before the Kr seeding. $\tau_{E,exp}/\tau_{E,ISS04}$ was ~ 0.8 which is 10% higher than

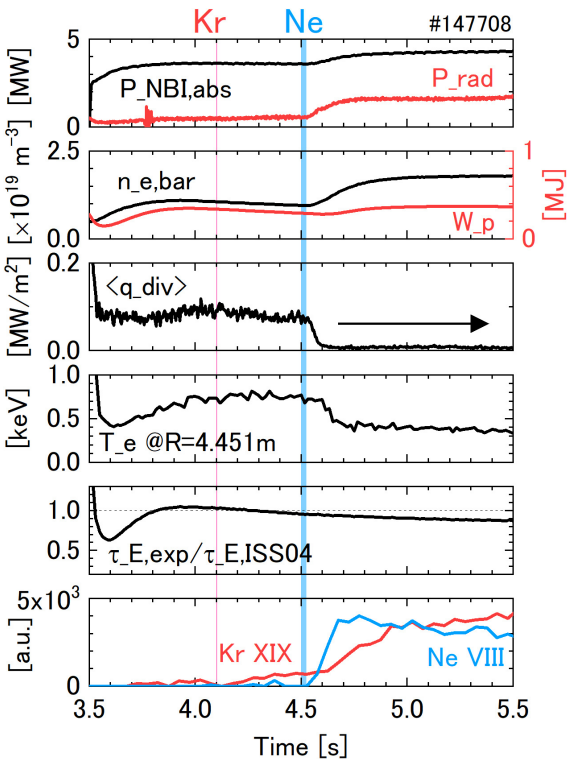


Fig. 6 Divertor detachment using Kr+Ne superimposed seeding. $f_{rad} \sim 40\%$ and 90% decreased $\langle q_{div} \rangle$ were sustained for $\sim 1$ s. $\tau_{E,exp}/\tau_{E,ISS04}$ was 10% higher than the Ne only seeding case. Pre-seeded Kr emission was drastically enhanced after Ne seeding.

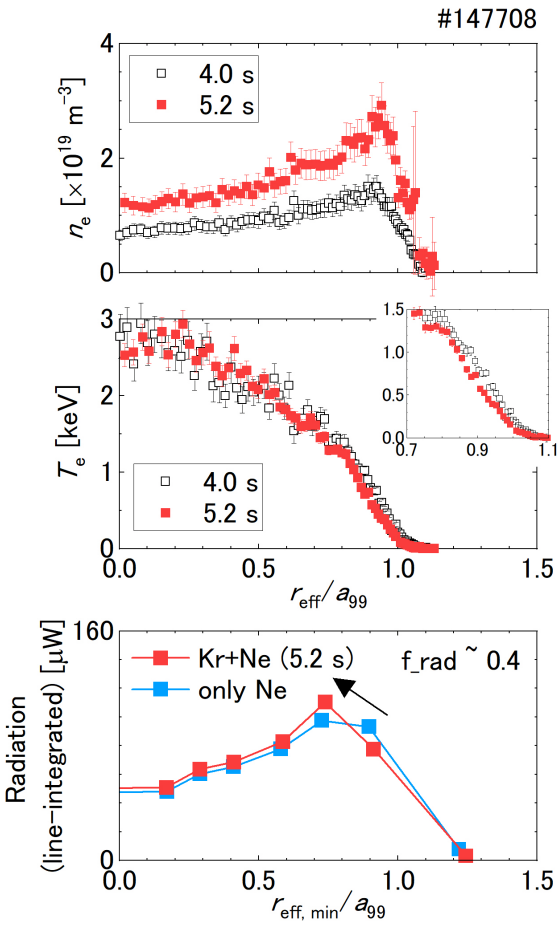


Fig. 7 After Kr+Ne seeding, $T_e$ locally decreased at $|r_{eff}/a_{99}| > 0.8$ while the $n_e$ profile shape was not changed. The radiation region moved upstream with the suppression of impurity accumulation toward the central plasma compared with the same $f_{rad}$ using Ne only seeding.

that with only Ne seeding as shown in Fig. 1. Kr emission remains very low until the Ne seeding, which then triggers KrXIX to increase together with NeVIII. Here, a clear decrease in $T_e$ at $|r_{eff}/a_{99}| > 0.8$ was observed due to the Ne seeding as shown in Fig. 7. $r_{eff}$ of $n_e$ and $T_e$ profiles is effective minor radius in Thomson scattering measurement. The line-integrated value of radiation profile is described using the minimum of effective minor radius, $r_{eff,min}$. Therefore, Kr could penetrate deeper than only Kr seeding. Radiation profile measurements show that radiation at $|r_{eff,min}/a_{99}| \sim 0.7$ in Kr+Ne seeding was larger than the radiation with only Ne seeding under the same $f_{rad} \sim 0.4$. It indicates that plasma radiation was successfully enhanced in the upstream region at the edge plasma using multi-species seeding compared with the case of single species seeding. Moreover, the radiation profile in Kr+Ne seeding implies that impurity accumulation toward the central plasma could be suppressed with the sustainment of the detachment.

## 5. Summary

In this paper, divertor detachment using Kr and Ne superimposed seeding on LHD was described. Multi-species impurity seeding is proposed to enhance plasma radiation not only in the divertor region but also in the upstream region with suppression of dilution for the management of the huge power exhaust in fusion devices.

Using only Ne seeding, the strongest $P_{rad}$ enhancement and $\langle q_{div} \rangle$ reduction were achieved. However, the detachment was short-lived due to the impurity screening at the ergodic layer. Using only Kr seeding, the plasma response was much slower and $P_{rad}$ enhancement was quite small. It can be considered that Kr atoms are ionized in the more downstream region in the ergodic layer where the friction force is dominant since Kr has a lower first ionization energy compared with Ne.

Kr and Ne superimposed seeding could overcome the limitation of the higher-Z seeding. $\langle q_{div} \rangle$ reduction which is comparable with only Ne seeding could be sustained for $\sim 1$ s. The plasma radiation was successfully enhanced in the upstream region at the edge plasma compared with the case of Ne seeding. This enhancement cannot be realized using Kr only seeding. It indicates the availability of multi-species impurity seeding with different cooling rate. These results are beneficial to improve the plasma

detachment scenario in fusion reactors. Further extension of the detachment will be conducted by optimization of the amount, flow rate and species of impurities. The effect of radial electric field on the impurity accumulation also should be investigated.

## Acknowledgments

The authors thank the LHD technical staff for their excellent support in the LHD experiments. This work was supported by JSPS KAKENHI Grant Number 17K14900 and by NIFS/NINS (NIFS16ULHH038, NIFS16UMLG701, NIFS16ULGG801).

[1] K. Gałązka *et al*., Contrib. Plasma Phys. **58**, 751 (2018).
[2] R. Zagórski *et al*., Nucl. Fusion **57**, 066035 (2017).
[3] S. Masuzaki *et al*., J. Nucl. Mater. **438**, S133 (2013).
[4] K. Mukai *et al*., Nucl. Fusion **55**, 083016 (2015).
[5] H. Tanaka *et al*., Nucl. Mater. Energy **12**, 241 (2017).
[6] C. Suzuki *et al*., Nucl. Mater. Energy **14**, 195 (2019).
[7] M. Kobayashi *et al*., Nucl. Fusion **59**, 096009 (2019).
[8] G. Kawamura *et al*., Plasma Phys. Control. Fusion **60**, 084005 (2018).
[9] H. Yamada *et al*., Nucl. Fusion **45**, 1684 (2005).
[10] H. Zhang *et al*., Jpn. J. Appl. Phys. **54**, 086101 (2015).